

Supplementary file

**Enhanced Thermoelectric Performance $\text{Bi}_{0.5}\text{Sb}_{1.5}\text{Te}_3/\text{SiC}$
Composites Prepared by Low-Temperature Liquid Phase
Sintering**

Bo Zhu,^{1,2,5} Yi Luo,¹ Haiyi Wu,¹ Du Sun,¹ Luo Liu,¹ Shengcheng Shu,³ Zhongzhen Luo,⁴ Qiang Zhang,^{2*} Ady Suwardi,^{6,7*} and Yun Zheng^{1*}

¹ Key Laboratory of Optoelectronic Chemical Materials and Devices, Ministry of Education, Jiangnan University, Wuhan 430056, China

² Key Laboratory of Interface Science and Engineering in Advanced Materials, Ministry of Education, Taiyuan University of Technology, Taiyuan 030024, China

³ Zhejiang Key Laboratory of Marine Materials and Protective Technologies, Zhejiang Key Laboratory of Marine Materials and Protective Technologies, Ningbo Institute of Materials Technology and Engineering (NIMTE), Chinese Academy of Sciences, Ningbo 315201, China

⁴ Key Laboratory of Eco-Materials Advanced Technology, College of Materials Science and Engineering, Fuzhou University, Fuzhou, 350108, China

⁵ The Institute of Technological Sciences, Wuhan University, Wuhan 430072, China

⁶ Institute of Materials Research and Engineering, Agency for Science, Technology and Research (A*STAR), Singapore 138634, Singapore

⁷ Department of Materials Science and Engineering, National University of Singapore, Singapore 117575, Singapore

*Corresponding authors: zhangqiang@tyut.edu.cn(Q.Z.); ady_suwardi@imre.a-star.edu.sg (A.S.); zhengyun@jhun.edu.cn (Y.Z.)

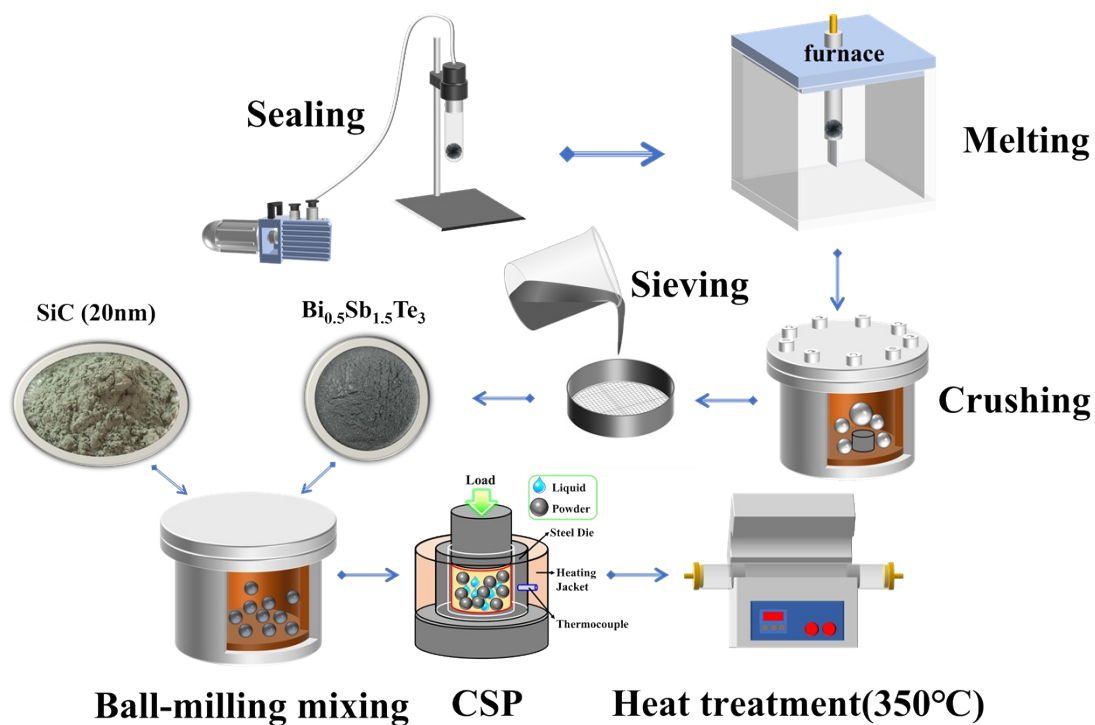


Figure S1. Schematic diagram of the sample synthesis process.

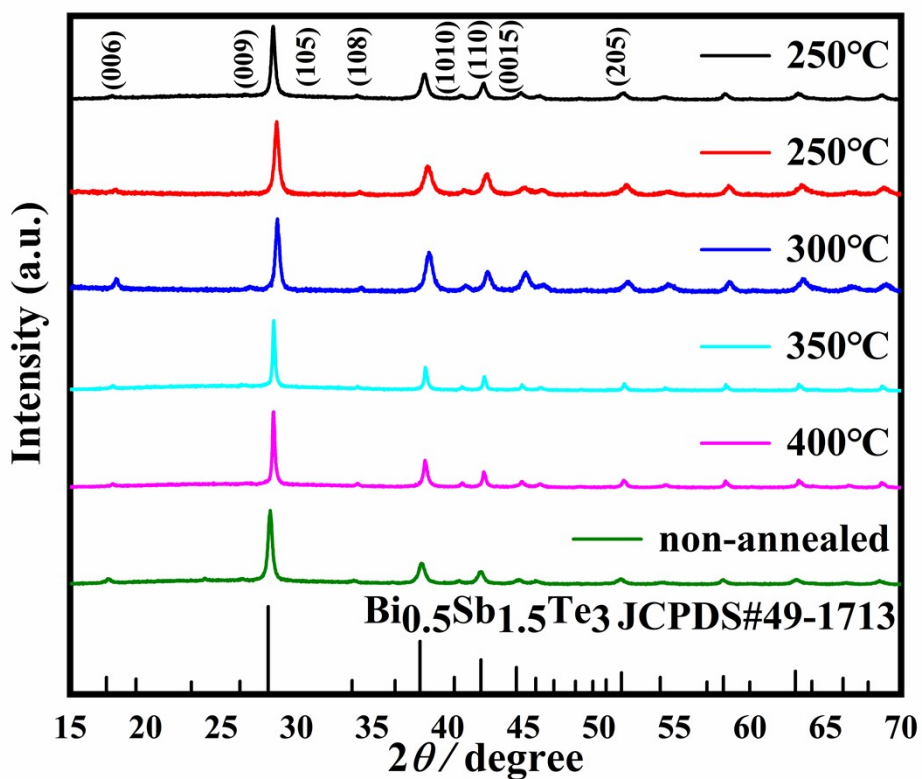


Figure S2. XRD patterns of $\text{Bi}_{0.5}\text{Sb}_{1.5}\text{Te}_3$ samples at different heat treatment temperatures.

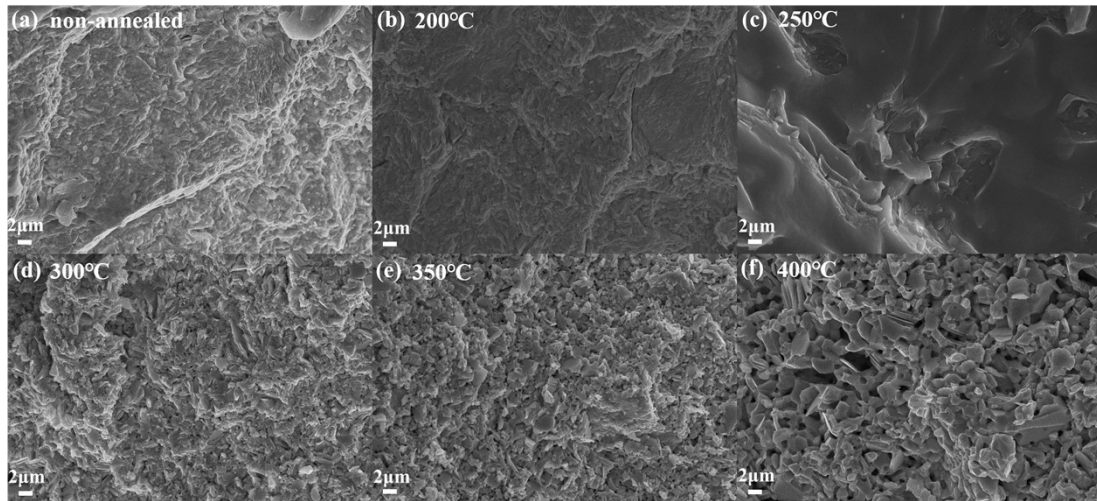


Figure S3. Fracture morphologies of Bi_{0.5}Sb_{1.5}Te₃ materials under different heat treatment conditions (a) non-annealed, (b) 200°C, (c) 250°C, (d) 300°C, (e) 350°C, (f) 400°C

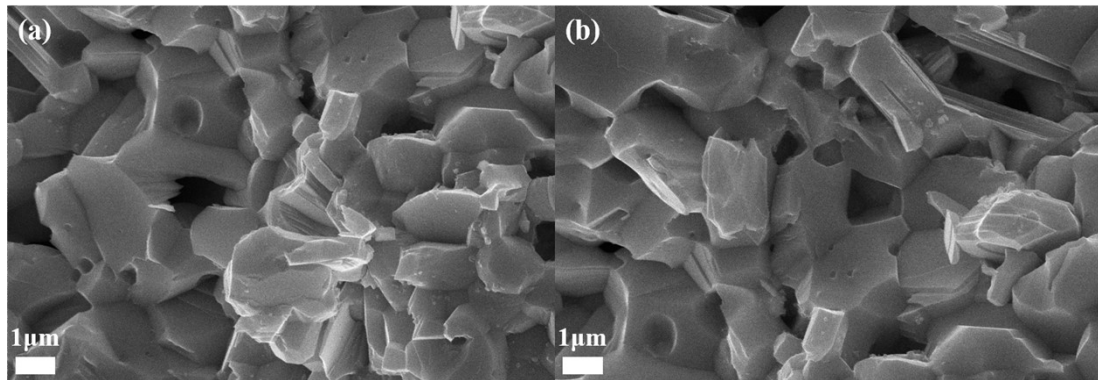


Figure S4. High-magnification SEM image of (a) 350 °C and (b) 400°C treated samples.

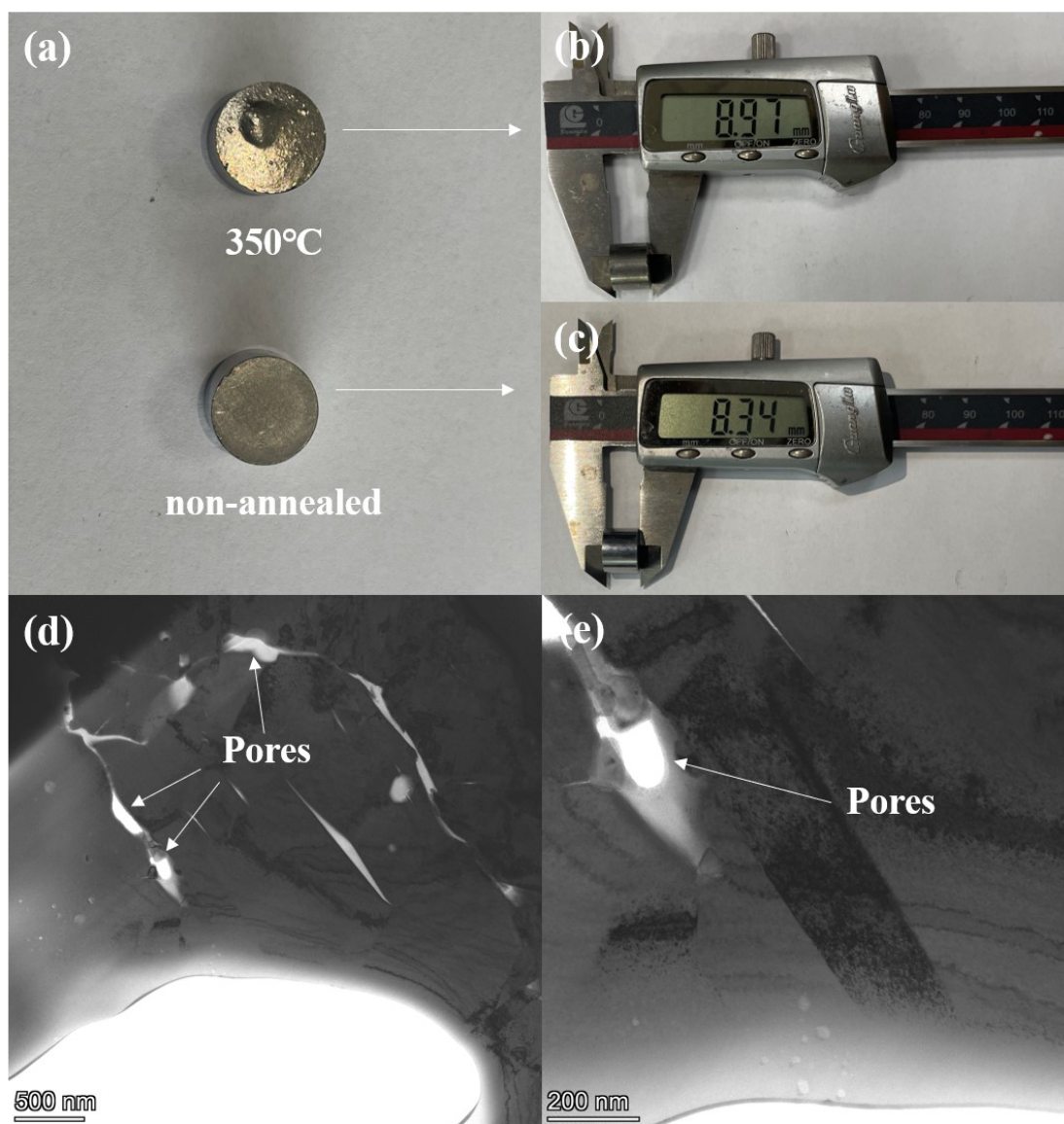


Figure S5. (a) Photos of 350 °C heat-treated and non-annealed samples. Heights of the same bulk sample (b) before and (c) after heat treatment at 350 °C. (d) and (e) Bright-field TEM images for the sample heat-treated at 350 °C. Arrows indicate pores in the sample.

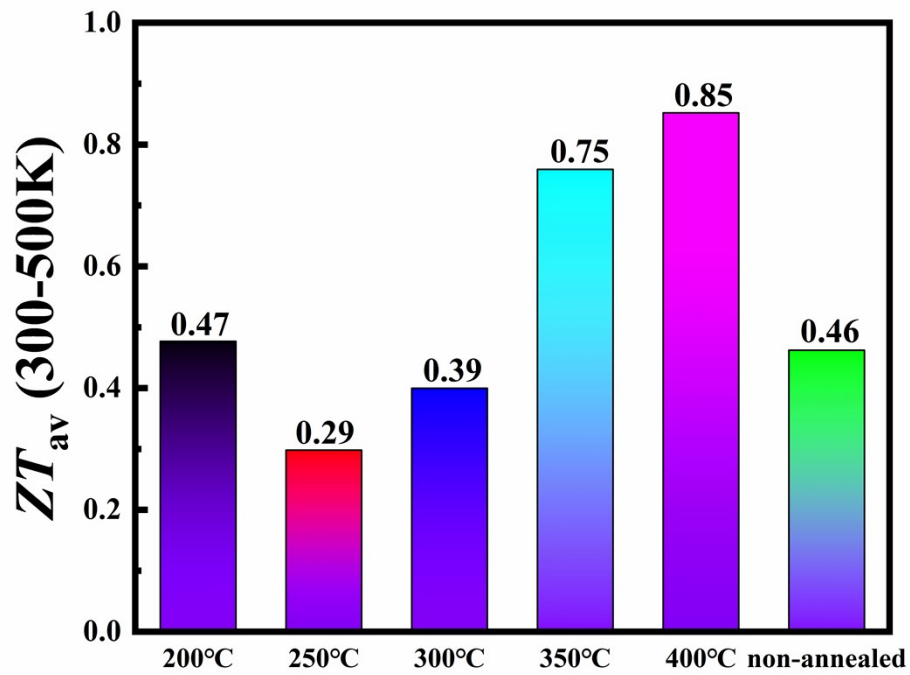


Figure S6. Temperature dependent average ZT values for samples heat-treated at different temperatures.

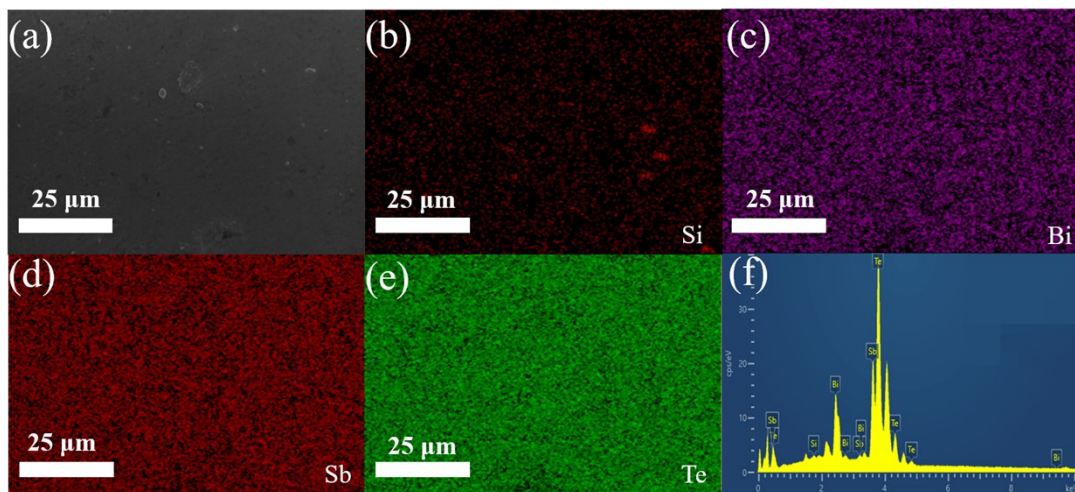


Figure S7. (a) The EDS mapping of $\text{Bi}_{0.5}\text{Sb}_{1.5}\text{Te}_3/x\text{vol}\% \text{SiC}$ ($x=0.6$), (b-e) The distribution of Si, Bi, Sb and Te element, (f) EDS composition of $\text{Bi}_{0.5}\text{Sb}_{1.5}\text{Te}_3/x\text{vol}\% \text{SiC}$ ($x=0.6$)

element	Wt%	wt% Sigma	At%
Si	0.24	0.05	1.16
Sb	28.27	0.26	30.91
Te	55.15	0.29	57.53
Bi	16.34	0.26	10.40
summation	100.00		100.00

Figure S8. EDS Quantitative Results

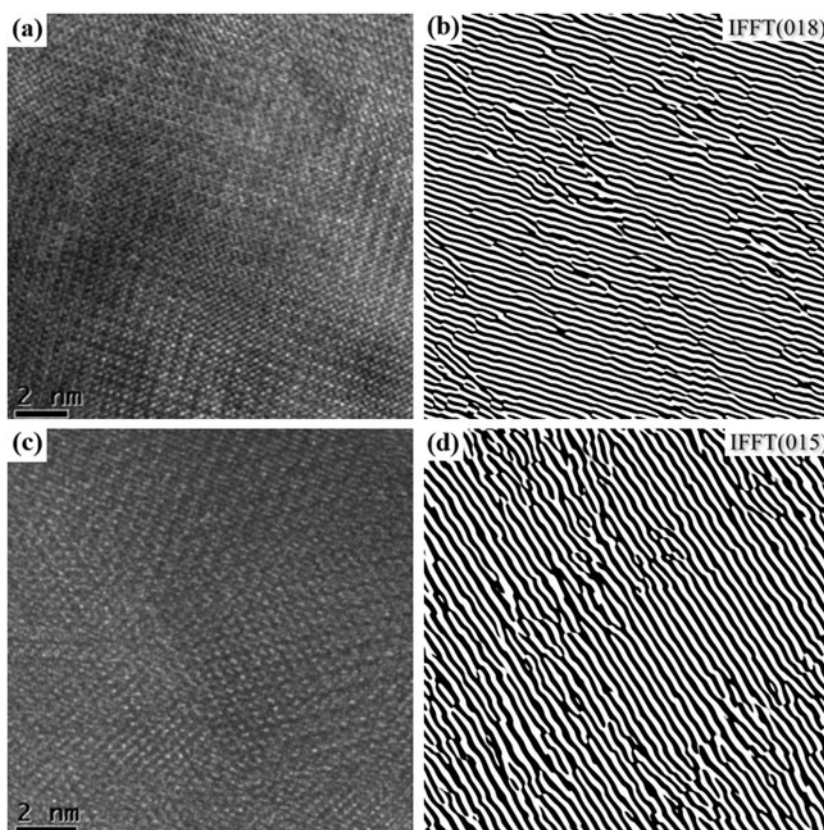


Figure S9. High-resolution TEM images of (a) $x = 0$ and (c) $x = 0.6$ samples; Inverse FFT images of (b) $x = 0$ sample on the (018) crystal plane and (d) $x = 0.6$ sample on the (015) crystal plane, respectively.

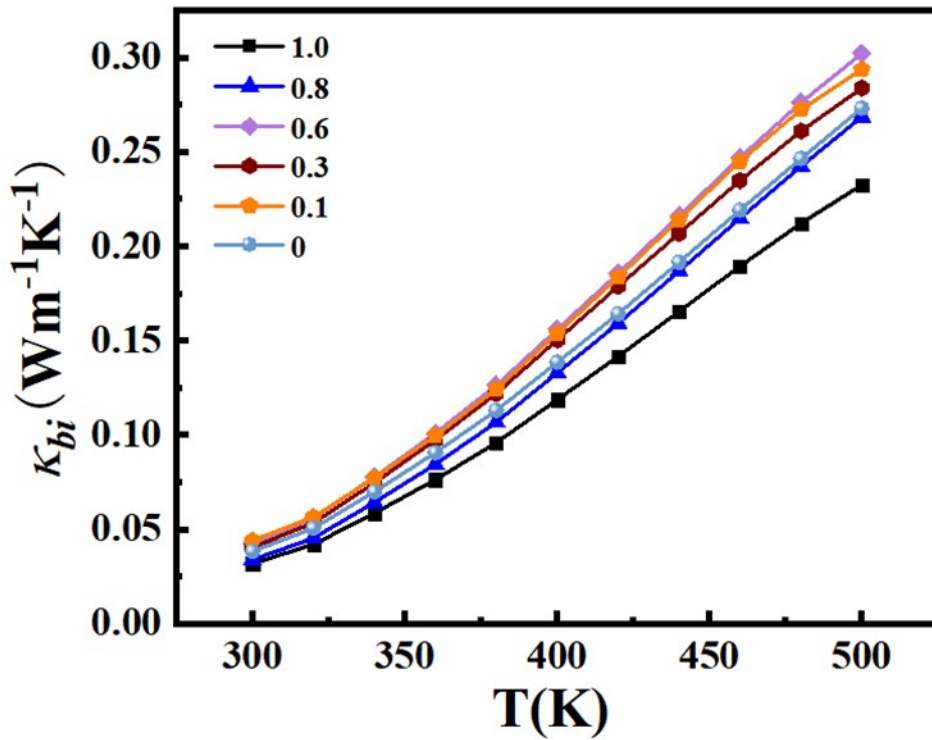


Figure S10. Temperature dependent bipolar thermal conductivity for $\text{Bi}_{0.5}\text{Sb}_{1.5}\text{Te}_3/x$ vol% SiC ($x=0, 0.1, 0.3, 0.6, 0.8,$ and 1.0) composite samples.

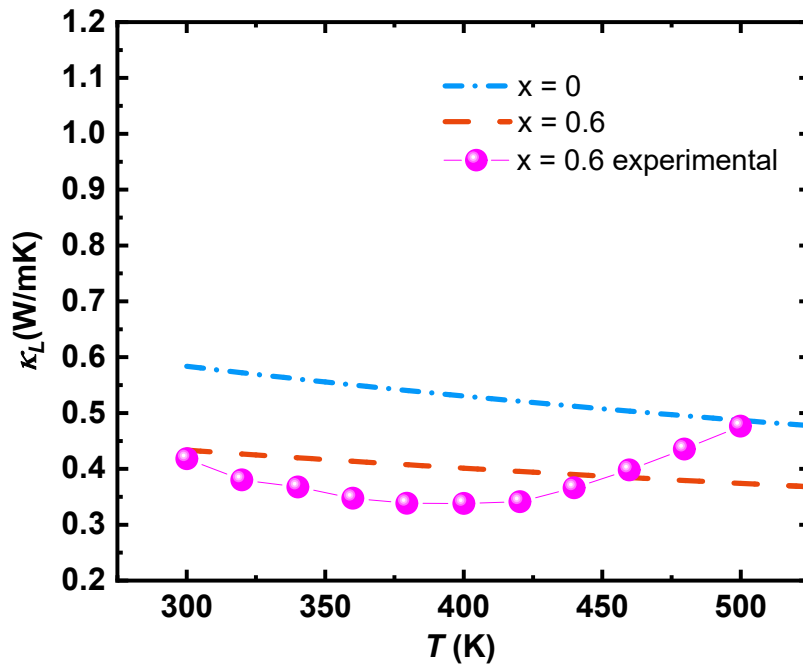


Figure S11. Debye-Callaway modelled lattice thermal conductivity for $x = 0$ and $x = 0.6\%$ compared to experimental values. The diameter of SiC nanoparticles is taken to be 20 nm based on Figure 12.